Nondestructive Testing and Evaluation Journal, Thomson Press Ltd., Accepted for publication

NDE of Composites Using Leaky Lamb Waves (LLW)

Yoseph Bar-Cohen[1], Shyh-Shiuh Lih[1], and Ajit K. Mal[2]

1 Jet Propulsion Laboratory, Caltech, MS 82-105, 4800 Oak Grove Dr., Pasadena, CA 91109, e-mail: yosi@jpl.nasa.gov, web: http://ndeaa.jpl.nasa.gov
2 Mechanical and Aerospace Engineering Department, University of California, Los Angeles, CA 90095, ajit@ucla.edu

ABSTRACT

The leaky Lamb wave (LLW) technique is approaching a maturity level that is making it an attractive quantitative NDE tool for composites and bonded joints. Since it was first observed in 1982, the phenomenon has been studied extensively, particularly in composite materials. The wave is induced by oblique insonification using a pitch-catch arrangement and the resulting modes are acquired by identifying minima in the reflected spectra. These modes are documented in the form of dispersion curves, which are evaluated in relation to analytical data. The wave behavior in multi-orientation laminates has been well documented and corroborated experimentally with high accuracy. The sensitivity of the wave to the elastic constants of the material and to the boundary conditions led to the capability to measure the elastic properties of bonded joints. Recently, the authors significantly enhanced the experimental capability that is associated with the LLW technique by increasing the speed of the data acquisition and the number of modes that can be identified. This capability enables greater accuracy of the data inversion as well as improves the flaw characterization. In spite of the theoretical and experimental progress, methods that employ oblique insonification of composites are still not being applied as standard industrial NDE. The authors investigated the possible causes that are hampering the transition of the LLW to industrial application and identified several key issues. The analytical and experimental capabilities at the current stage are reviewed and the issues that are affecting the transition of the technique to practical use are described in this paper.

KEY WORDS: Leaky Lamb Waves (LLW), NDE, Composites, Stiffness Constants, Plate Wave Modes

LEAKY LAMB WAVE PHENOMENON

The Leaky Lamb wave (LLW) phenomenon is induced when a pitch-catch ultrasonic setup insonifies a plate-like solid immersed in fluid. This phenomenon was discovered while testing a composite laminate using a Schlieren imaging system (Figure 1) [Bar-Cohen, et. al, 1993]. The phenomenon is associated with the resonant excitation of plate waves that leak energy into the coupling fluid and interfere with the specular reflection of the incident waves. The destructive interference between the leaky waves and the specularly reflected waves modifies the reflected spectrum introducing a series of minima in the spectra of the reflected waves. The LLW experiment for composite laminate specimens involves measurement of the reflected field and extraction of the minima in the reflected spectra at various angles of incidence and orientations (polar angles) with respect to the laminate. The data is presented in the form of dispersion curves showing the phase velocity (calculated from Snell's law and the angle of incidence) of the

leaky Lamb waves as a function of frequency. The sensitivity of the dispersion curves to variations in the properties of the composite material, namely its anisotropy, layers thickness, stiffness constants, and the presence of defects, has made this phenomenon an attractive NDE method.

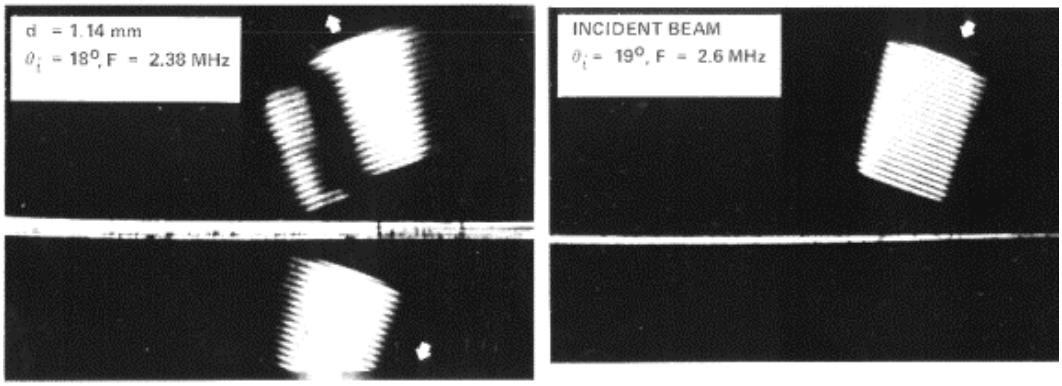

FIGURE 1: A Schlieren image of the LLW phenomenon showing a tone-burst before (right) and after impinging on a graphite/epoxy laminate.

Bar-Cohen and Chimenti [1984] investigated the characteristics of the LLW phenomenon and its application to NDE, focusing on the experimental documentation of observed modes and the effects of various types of defects on the measurements. Their study was followed by numerous theoretical and experimental investigations of the phenomenon [e.g., Nagy, et al, 1987, Nayfeh & Chimenti, 1988, Mal & Bar-Cohen, 1988, Rohklin, et al, 1989, Dayal & Kinra, 1989, Balasubramanian & Rose, 1991, Jansen & Hutchins, 1992]. A method was also developed to invert the elastic properties of composite laminates from the LLW dispersion data [Mal, 1988; Mal & Bar-Cohen, 1988; and Shih, et al, 1998] and the study was expanded to the NDE of bonded joints [Bar-Cohen, et al, 1989].

The experimental acquisition of dispersion curves for composite materials requires accurate control of the angle of incidence/reception and the polar angle with the fibers. To perform these measurements rapidly and accurately, a LLW scanner was designed and constructed by Bar-Cohen, et al, [1993] in collaboration with QMI (Costa Mesa, CA). With the aid of a personal computer, the scanner controls the height, angle of incidence and polar angle of the pitch-catch setup. It also manipulates the angle of incidence/reception simultaneously while maintaining a pivot point on the specimen surface.

A photograph of the scanner installed on a C-scan unit is shown in Figure 2. A computer code was written to control the incidence and polar angles, the height of the transducers from the sample surface, and the transmitted frequency. The data acquisition involves the use of sequentially transmitted tone-bursts, each of a specific frequency, spanning a selected frequency range (within 20dB level of the transducer pair). The reflected signals are acquired as a function of the polar and incidence angles and saved in a file for analysis and comparison with theoretical predictions. The minima in the acquired reflection spectra represent the LLW modes and are used to determine the dispersion curves (phase velocity as a function of frequency). The incident angle is changed incrementally within the selected range and the reflection spectra are acquired. For graphite/epoxy laminates the modes are identified for each angle of incidence in the range of 12^o to 50^o allowing the use of free-plate theoretical calculations. At each given incidence angle, the

minima are identified, added to the accumulating dispersion curves, and plotted simultaneously on the computer display. While the data acquisition is in progress, the acquired minima are identified on both the reflected spectra and the dispersion curves.

FIGURE 2: A view of the LLW scanner (bridge right side) installed on the JPL's C-scan system.

A follow-on study by Bar-Cohen, et al, [1991] showed that the capability to invert the elastic properties using LLW data is limited to the matrix-dominated stiffness constants. This limitation can be partially overcome if the incidence angles of 10^o or smaller can be used in the experiments, but this is difficult if not impossible to achieve in practice with a single scanner. An alternative methodology based on pulsed ultrasonics was developed by Bar-Cohen, Mal and Lih [1993]. Using pulses in pitch-catch and pulse-echo experimental, it was shown that all five elastic constants of a unidirectional laminate could be determined with a fairly high degree of accuracy. This chapter provides a summary of the analytical model, the experimental procedure and test results used in he LLW method. It also discusses the challenges that need to be overcome in order to transfer the technology to practical applications.

LLW THEORY AND DATA INVERSION

Plate wave theory

The behavior of ultrasonic waves propagating through fiber-reinforced composites is determined by the material stiffness and dissipative characteristics. Theoretical modeling of this behavior requires several simplifying assumptions regarding the properties of the material. First, the unidirectional bulk material is treated as homogeneous, since the fiber diameter (e.g., graphite 5-10 μm and glass 10-15 μm) is significantly smaller than the wavelength (for frequencies up to 20 MHz the wavelength is larger than 100 μm). Each layer of a composite laminate is assumed to be transversely isotropic, bonded to its neighboring layers with a thin layer of an isotropic resin at their interfaces. The mechanical behavior of the material of each lamina is described by an ensemble average of the displacements, the stresses and the strains over a representative volume element [Christensen, 1981]. The average strains are related to the average stresses through the effective elastic moduli. As a transversely isotropic material, unidirectional fiber-reinforced composites are characterized by five independent effective stiffness constants c_{ij}. These constants dependent on the elastic properties of the fiber and matrix materials as well as their volume fraction. The stress components, s_{ij} are related to the strain components e_{ij} through a linear constitutive equation. For a transversely isotropic elastic solid with its symmetry axis along the x_1-axis this equation can be expressed in the form [Mal and Singh, 1991],

$$\begin{Bmatrix} s_{11} \\ s_{22} \\ s_{33} \\ s_{23} \\ s_{31} \\ s_{12} \end{Bmatrix} = \begin{bmatrix} c_{11} & c_{12} & c_{12} & 0 & 0 & 0 \\ c_{12} & c_{22} & c_{23} & 0 & 0 & 0 \\ c_{12} & c_{23} & c_{22} & 0 & 0 & 0 \\ 0 & 0 & 0 & c_{44} & 0 & 0 \\ 0 & 0 & 0 & 0 & c_{55} & 0 \\ 0 & 0 & 0 & 0 & 0 & c_{55} \end{bmatrix} \begin{Bmatrix} e_{11} \\ e_{22} \\ e_{33} \\ 2e_{23} \\ 2e_{13} \\ 2e_{12} \end{Bmatrix} \tag{1}$$

where the five independent stiffness constants of the material are c_{11}, c_{12}, c_{22}, c_{23}, c_{55}, and

$$c_{44} = \tfrac{1}{2}(c_{22} - c_{23})$$

Calculation of the effective elastic constants of composite materials has been the topic of many studies. Extensive discussions of the bounds for the effective elastic moduli of fiber-reinforced composites can be found in [Christensen, 1981] and other associated literature cited therein. For low frequencies and low fiber concentration, the theoretical prediction of the effective elastic constants is in good agreement with experimental results. On the other hand, for high frequencies the theoretical estimates are not satisfactory since the effect of wave scattering by the fibers becomes significant. For fiber-reinforced composite materials, dissipation of the waves is caused by the viscoelastic nature of the resin and by multiple scattering from the fibers as well as other inhomogeneities. Both dissipation effects can be modeled by assuming that the stiffness constants, $c_{ij,}$ are complex and frequency-dependent [Mal, et al, 1992]. Since the effects of dissipation on the velocity of the waves is usually quite small, the material is often assumed to be perfectly elastic in the application of the LLW technique.

The geometry of the general theoretical problem is shown in Figure 3, where a plane acoustic wave is incident on a composite laminate immersed in a fluid. The thickness of the fluid layers above and below the specimen is large compared to the wavelength and the thickness of the laminate, so that they can be assumed to be semi-infinite. The interaction of the ultrasonic waves with the plate excites a variety of elastic waves including reflected and transmitted body waves and multimode guided waves. All of these waves are affected by the properties of the material as well as the nature of the interfaces. Some of their characteristics can be extracted from the reflected and transmitted wave data that is acquired as a function of frequency and angle of incidence through comparison with theoretical results.

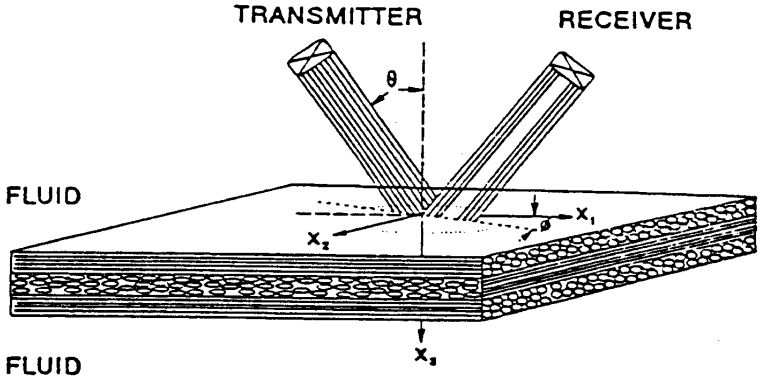

FIGURE 3: The general theoretical problem associated with the LLW method.

Application of the LLW technique to the NDE of composite structures requires theoretical calculation of the Lamb wave dispersion curves for a given model of laminates that are often used to construct these structures. A number of authors have dealt with this problem [see, e.g., Nayfeh and Chimenti, 1988; Mal and Bar-Cohen, 1988] and have developed efficient and accurate computer codes for generating the dispersion in presence or absence of the surrounding fluid. The effect of fluid loading has been found to be negligible at incident angles and frequencies of interest in most applications. For a homogeneous but anisotropic plate the dispersion curves are obtained through the solution of an equation of the form

$$G(v, f, n_i, c_{ij}, r, h) = 0$$

where v is the phase velocity of the guided waves at frequency, f, along the direction vector, $\boldsymbol{n}$, on the plate surface, c_{ij} is the elastic tensor and r is the density of the material, and h is the plate thickness. The dispersion function, G, is obtained from the solution of the boundary value problem depicted in Figure 3. It should be noted that for a given value of v, there are multiple values of f associated with different modes of propagation of the Lamb waves in the plate, and these frequencies correspond to the minima in the reflected spectra for a given incident angle.

For a multilayered laminate with n layers, each of the material constants, c_{ij}, r, and h is a vector of dimension n. At low frequencies, where the wavelengths are long compared to the total plate thickness, it is possible to develop approximate theories based on kinematic assumptions regarding the variation of the strains across the thickness of the plate. The approximate dispersion equation is of the form

$$G\ (v, f, n_i, b_{ij}, r\ ) = 0 \qquad (2)$$

where b_{ij}'s are the in-plane laminate stiffness constants. They are related to the material stiffness constants, c_{ij}, and the thickness of the layers. For a symmetric cross-ply laminate, there are three independent components of b_{ij}, namely, b_{11}, b_{12} and b_{66}. The values of these constants can also be determined form low frequency LLW or other ultrasonic methods. [Shih, et al, 1998].

The Simplex Algorithm

The locations of the minima in the spectra of the reflected waves have been found highly sensitive to the thickness and the stiffness constants of the plate and are relatively insensitive to the damping parameters as well as the presence of water in a broad frequency range. Thus the dispersion data can, in principle, be used to determine accurately these properties and any changes in their values during service. The phase velocity of guided waves in a composite laminate in absence of water loading is obtained from the theoretical model as a transcendental equation and its function requires minimization. The minimization can be carried out through a variety of available optimization schemes. We have used the Simplex algorithm, which is based on a curve-fitting technique for a given set of data points to any function, no matter how complex. We illustrate the basic concept behind the method through its application to a simple function first.

Let us consider a function *f* of two variables *x* and *y*, and two unknown parameters *a* and *b*:

$$f(a,b;x,y) = 0$$

Let us assume that there are a total of *n* data sets, x_i, y_i, i = 1, 2, ... *n*. Since the data sets are not exact, the error, e_i associated with the i^{th} set is given by

$$e_i = f(a,b;x_i,y_i)$$

An objective function is defined in the form

$$S = \sum_{i=1}^{n} w_i \cdot e_i \qquad (3)$$

where w_i is a statistical weight. Now, the problem of curve fitting becomes the problem of finding a set of the parameters *a* and *b* that yields the minimum value of *S*.

A simplex algorithm is a geometric figure that has one more vertex than the dimension of the space in which it is defined. For example, a simplex on a plane (a two-dimensional space) is a triangle; a simplex in a three-dimensional space is a tetrahedron, and so on. Returning to the simple example, we build a plane with *a* and *b* as the two axes; then create a simplex (a triangle) as shown in the Figure 4. Each vertex of the triangle is characterized by three values: *a*, *b* and *S*.

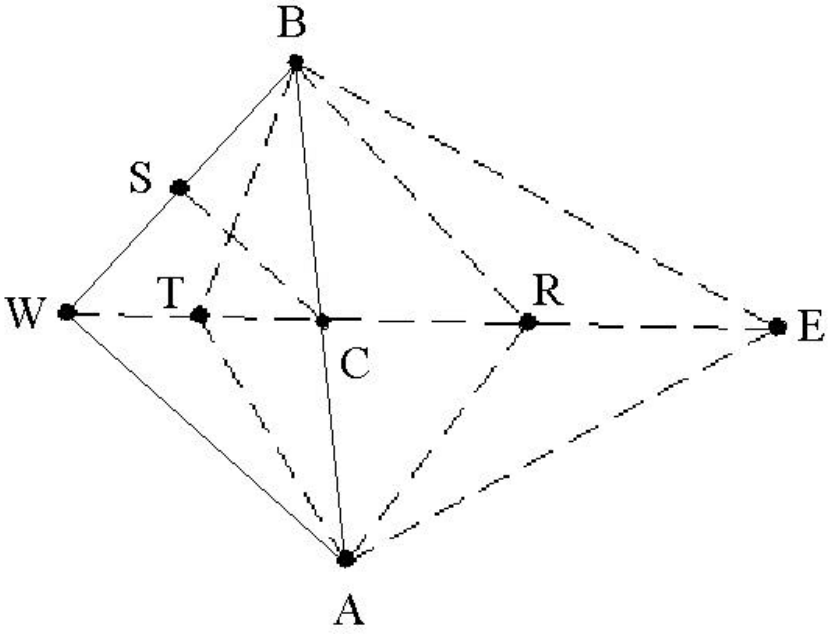

FIGURE 4: A 2-D simplex BWO illustrating the four mechanisms of movement: reflection, expansion, contraction, and shrinkage. B = best vertex, W = worst vertex, R = reflected vertex, E = expanded vertex, C = contracted vertex, and S = shrinkage vertexes.

To reach the minimum value of *S*, the following rules are used: find which vertex corresponds to the highest (worst) and which to the lowest (best) values of *S*, then reject the worst vertex and replace it with another vertex. Four mechanisms are used to find the new vertex: reflection,

expansion, contraction, and shrinkage. If d be the distance from the worst vertex to M, the midpoint of all the other vertices, then the reflected vertex is located at a distance d from M on the line continuation that joins the rejected vertex to M. The response of the reflected vertex is calculated and compared to the responses of previous set of vertices. The procedure can be divided into three groups as follows:

- The reflected vertex has a lower (better) response than the previous best. Then the expanded vertex (by reflecting twice the distance d) is tested. The expanded vertex is accepted if it has a lower response than the rejected one; otherwise the reflected one is accepted.
- The reflected vertex has a higher (worse) response than the rejected vertex. Then the contracted vertex (by moving the rejected one a distance of one-half d toward the midpoint M) is tested. This contracted vertex is accepted if it produces a better (lower) response than the rejected one; otherwise, a shrinkage occurs and all vertexes, except the best one, move directly toward it by half of their original distance from it.
- The reflected vertex has a response better than the rejected one and worse than the best one. Then this reflected vertex is accepted.

These four mechanisms are illustrated in the Figure 4. The above steps are repeated until satisfied convergence is achieved. The locations of the minima in the reflection coefficients are highly sensitive to the thickness and the stiffness constants of the plate and are insensitive to the damping parameters as well as the presence of water in a broad frequency range. Thus the dispersion data can, in principle, be used to determine accurately these properties and any changes in their values during service. Other details of the inversion process can be found in [Karim et al, 1990], and will not be repeated here. It should be noted that the simplex method is extremely efficient for the data inversion problem associated with the LLW technique.

The phase velocity of guided waves in a composite laminate in absence of water loading is obtained from the theoretical model as a transcendental equation given in equations (2) and (3). For a given data set $\{f_k, v_k\}$, c_{ij} and h can be determined by minimizing the objective function

$$F(c_{ij}, h) = \Sigma\, w_k \,|G_k|^2 \qquad (4)$$

where w_k is a suitable weight function and G_k is the value of the dispersion function G at the k-th data set.

Data Inversion

The experimental system used in our studies consists of an LLW scanner (shown schematically in Figure 5, which is computer controlled for changing the transducers' height, rotation angle and the angle of incidence. The LLW scanner is an add-on to standard ultrasonic scanning systems as shown photographically in Figure 2. The control of the angle of incidence allows simultaneous changes in the transmitter and receiver angles while maintaining a pivot point on the part surface and assuring accurate measurement of the reflected ultrasonic signals. The signals are transmitted by a function generator that frequency-modulates the required spectral range. This generator also provides a reference frequency marker for the calibration of data acquisition when converting the signal from time to frequency domain. A digital scope is used to acquire the reflection spectra after being amplified and rectified by an electronic hardware.

The signals that are induced by the transmitter are received, processed and analyzed by a personal computer after being digitized. As discussed earlier, the reflected spectra for each of the desired angles of incidence is displayed on the monitor and the location of the minima (LLW modes) are marked by the computer on the reflection spectrum. These minima are accumulated on the dispersion curve, which is shown in the lower part of the display in Figure 6. The use of the frequency modulation approach introduces a significant increase in the speed of acquiring the dispersion curves. In this approach 20 different angles of incidence can be acquired in about 45 seconds in contrast to over 15-minutes using the former approach. Once the dispersion data is ready, the inversion option of the software is activated and the elastic stiffness constants are determined as shown in Figure 6.

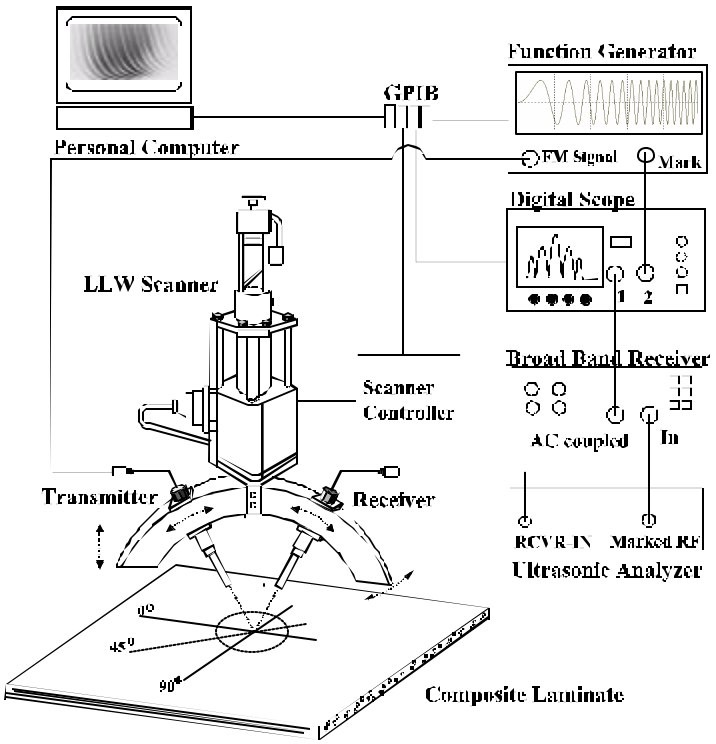

FIGURE 5: A schematic view of the rapid LLW test system.

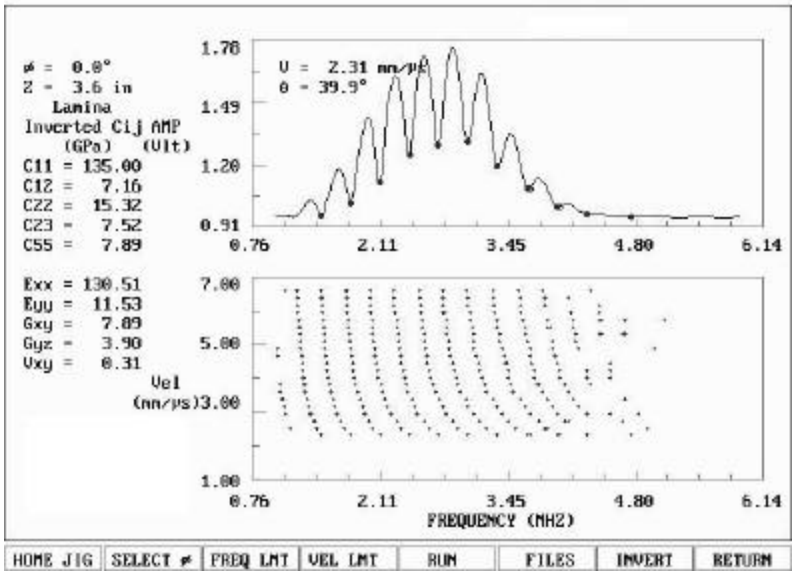

FIGURE 6: Computer display after the data acquisition and inversion completion. The elastic stiffness constants are inverted from the dispersion curve and are presented on the left of the screen.

Using the system with the enhanced data acquisition speed, various defects can be detected and characterized based on the quantitative data that is available from the dispersion curves. In Figure 7a, the response from a defect-free graphite/epoxy laminate tested at the 0-degree polar angle is shown. In Figure 7b, the response from an area with a layer of simulated porosity (microballoons) is presented. As expected, at low frequencies the porosity has a relatively small effect and the dispersion curve appears similar for the two cases. On the other hand, as the frequency increases, the porosity layer emulates a delamination and modifies the dispersion curves to appear as those for a laminate with half the thickness of the undamaged laminate.

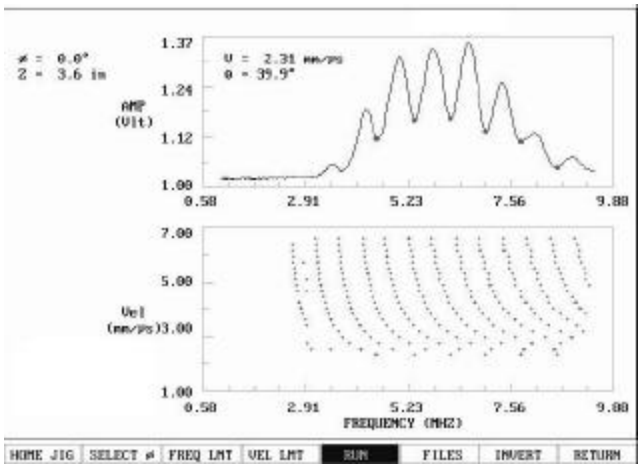

FIGURE 7a: The refection at 39.5 degrees incidence angle and the dispersion curve for a Gr/Ep $[0]_{24}$ laminate with no defects

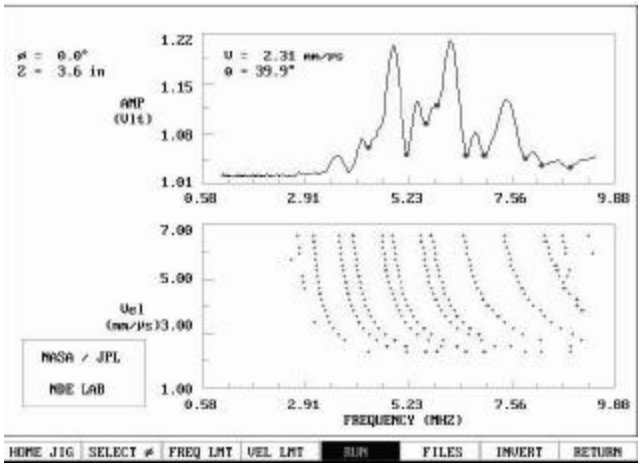

FIGURE 7b: The response at a defect area where simulated porosity was introduced in the middle layer using microballoons.

The LLW dispersion data and inverted results for a unidirectional graphite/epoxy plate were shown in Figure 6. The material is AS4/3501- 6 and the polar angle (i.e., the direction of Lamb wave propagation) is 0^o with respect the fibers. The reflected spectrum for 39.9^o incident angle is shown at the top of this Figure, and the accumulating dispersion curves are shown at the bottom. The inverted elastic and stiffness constants are given at the left.

The LLW method can also be used characterize materials degradation of composites. A sample made of AS4/3501-6 $[0]_{24}$ laminate was tested after it was subjected to heat treatment. The sample was exposed to a heat ramp from room temperature to 480^o F for 15 minutes, and then was taken out of the oven to cool in open air at room temperature. It was tested at a specific location before and after heat treatment. The measured dispersion curves for the two cases are shown in Figure 8. It can be seen that there are distinct differences in the dispersion data for the specimen before and after heat treatment. Since the heat damage occurs mostly in the matrix, the effect is expected to be more pronounced in the matrix dominated stiffness constants. The constants c_{11}, c_{12}, c_{22}, c_{23} and c_{55} obtained from the inversion process are 127.9, 6.32, 11.85, 6.92 and 7.43 GPa, before heat treatment, and 128.3, 6.35, 10.55, 6.9 and 7.71 GPa, after heat treatment. The most noticeable and significant change is in the stiffness constant c_{22}, which is the property most sensitive to the matrix, and it resulted in a significant reduction in the transverse Young's modulus.

It should be noted that the dispersion equation is strongly nonlinear in c_{ij} (stiffness matrix) and h (thickness), and its solution is non-unique. Thus, extreme care must be taken in interpreting the numerical results obtained from the inversion of the dispersion data. Extensive parametric studies of the inversion process have shown that only the thickness and the matrix dominated constants c_{22}, c_{23} and c_{55} can be determined accurately from the inversion of dispersion data. This is due to the fact that the dispersion function G is not very sensitive to the fiber dominated constants c_{11} and c_{12}. These two constants can be determined accurately from the travel times and amplitudes of the reflected short-pulse signals in the oblique insonification experiment [Bar-Cohen, Mal and Lih, 1993], to be discussed below. For a thin symmetric cross-ply laminate, the guided data must be supplemented with direct measurement of other wave speeds in order to determine all three in-plane laminate constants [Shih, Mal and Vemuri, 1998].

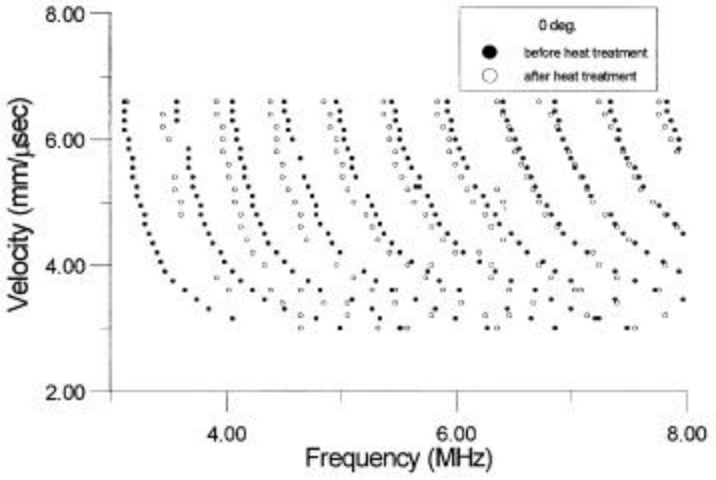

FIGURE 8: The measured dispersion curves of a $[0]_{24}$ graphite-epoxy panel before and after heat treatment.

DATA ACQUISITION

Extensive studies of composites by the present authors have led to the identification of a series of factors that affect reliability of the inversion and the transition of the technique to practical applications. The process of acquiring the spectrum was identified as one of these factors - it is time consuming and has a series of redundancies. Our recent efforts have concentrated on the enhancement of the speed of the data acquisition and the number of modes that can be identified in the LLW experiment.

One of our recent enhancements is the use of transmitted signals that have been modified to frequency-modulated pulses that are induced sequentially within the required spectral range. The specific signal consists of a time-dependent voltage function $V(t)$ that is amplified and transmitted at an induced frequency $f(t)$ of the form

$$f(t) = f_0 \times (1 + k_1)^{tk_2} \qquad (5)$$

where f_0 is initial frequency and the constants k_1, k_2 are the frequency parameters related to sampling time. A trigger based on the selected time window is transmitted to synchronize the reflected signals on the data acquisition scope, and the time domain signal is converted to spectral data using the above equation. The function generator also provides a reference

frequency marker for the calibration of the acquired data when converting the signal from time to frequency domain. A digital scope is used to acquire the reflection spectral data after being amplified and rectified by electronic hardware. The signals that are induced by the transmitter are received, digitized, processed and analyzed by a personal computer. The reflected spectra for each of the desired angles of incidence is displayed on the monitor, and the locations of the minima (LLW modes) are marked by the computer on the reflection spectrum. The algorithm used to identify the minima was modified to employ reliably smaller level signals, which are associated with more diffused modes. The identified minima are accumulated on the dispersion curve, which is shown on the lower part of the display (see Figure 6).

Optimal Adjustment of the Wave Propagation orientation

The direction of the wave propagation in relation to the fibers is important for quantitative evaluation of the test results. Generally, the top layer is used in the LLW studies as the reference orientation or as the 0^o layer. Visual adjustment of the orientation can lead to errors as high as $\pm 5^o$. In order to minimize this error, the polar backscattering that was discovered by the principal author [Bar-Cohen and Crane, 1982] was used to determine the direction of the first layer. The approach takes advantage of the fact that maximum backscattering is obtained from the fibers when insonifying the laminate within the plan that is normal to the fiber orientation. Practically, the transducer needs to be rotated about 200^o around an axis that is normal to the laminate and recording the amplitude of the backscattered signals while searching for the maximum value. A program that the authors wrote to search for the maximum amplitude provided about $\pm 0.1^o$ accuracy of the first layer orientation.

Optimal Adjustment of Transducers' Height

During Leaky Lamb Wave (LLW) experiments, the height of the transducer pair is an important issue. For best results, the crossing point of the beam from the two transducers must fall on the surface of the specimen. If this point is located outside the surface, the sharpness of the minima in relation to the adjacent data points becomes weaker as shown in Figure 9a. In such cases, the identification of the minima becomes difficult and increasingly inaccurate. To adjust the height of the transducers precisely and efficiently, an algorithm was developed and implemented into the computer control program for the LLW experiment. The algorithm optimizes the contrast of the minima by determining the maximum variations in the reflection spectrum using adaptive adjustment of the height of the transducer pair.

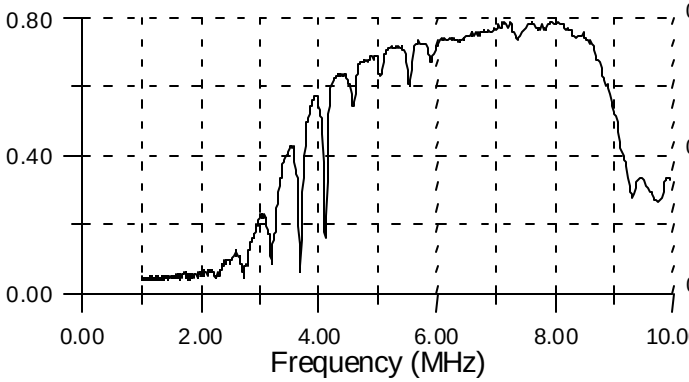

FIGURE 9A: "Out of focus" LLW reflection spectrum.

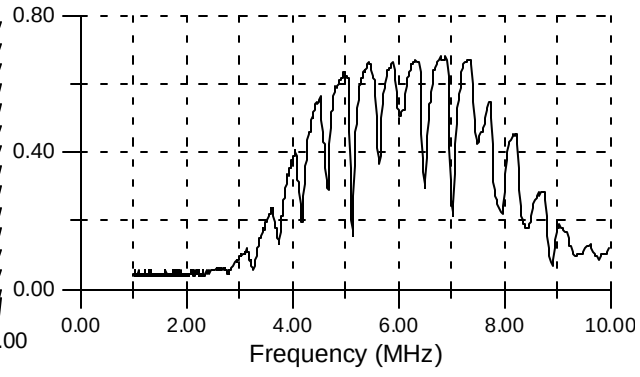

FIGURE 9B: Optimized reflection spectrum using adaptively adjusted transducers pair height.

Using this algorithm interactively with the LLW setup controller, an optimal and fine-tuned height of the transducer pair can be identified automatically. An example of the refinement is shown in Figure 9b.

As indicated earlier, the use of the frequency modulation and automatic optimal adjustment of the transducer height significantly increase the speed and accuracy of acquiring LLW dispersion curves.

DISPERSION CURVES WITH ENHANCED MODE IDENTIFICATION

To further enhance the accuracy of the dispersion data, a method has been developed to acquire and to display them as an image. Examples of such dispersion curves are shown in Figure 10a, and b for a 3.125 mm thick unidirectional laminate tested at 0^o and 45^o polar angles, respectively. This method has been found to allow viewing modes with amplitude levels that are significantly smaller than what has been observed before. The white curved lines show the modes of the dispersion curve. It can be seen in the case of propagation at 45^o to the fibers (Figure 10b), the modes that would otherwise be considered noise are clearly identified using this approach. To demonstrate the capability of this method further a 1.6 mm aluminum plate was tested in the low frequency region near the first symmetric and antisymmetric modes. As shown in Figure 11 the portion of the mode that is almost parallel to the frequency axis is identified clearly, offering a significant improvement over previous single frequency methods where it would be very difficult to generate these curves with such high accuracy.

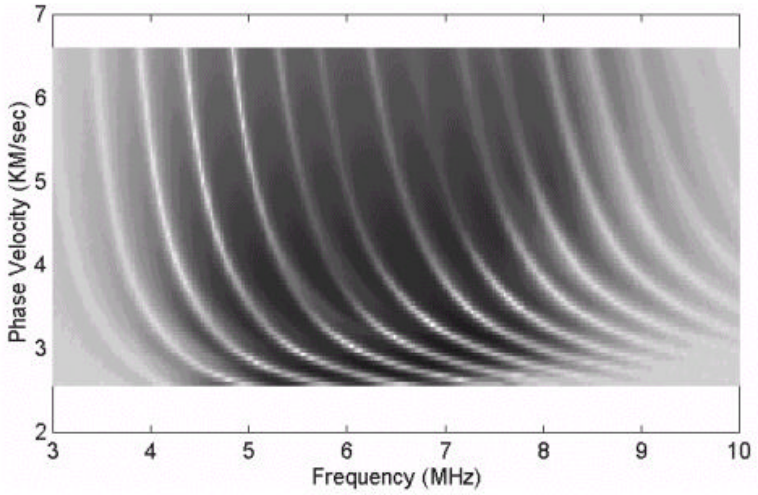

FIGURE 10a: A view of the LLW dispersion curve for a unidirectional Gr/Ep for wave propagation along the fibers generated by an imaging method.

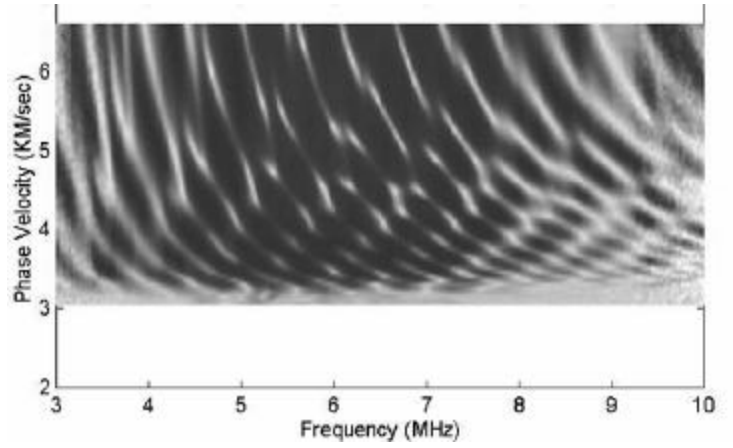

FIGURE 10b: Sam as in Fig 10a for propagation at 90^o to the fibers.

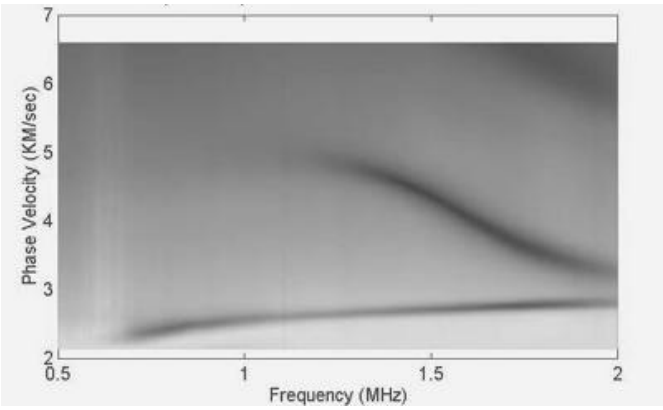

FIGURE 11: A view of the first symmetric and antisymmetric modes of Lamb wave dispersion curves in an aluminum plate using the imaging method.

PULSED OBLIQUE INSONIFICATION

Time-domain experiments in certain directions offer an alternative method to determine the elastic constants c_{ij} for unidirectional composites accurately and efficiently. The ray analysis of the various reflected waves in the leaky Lamb wave experiment for a unidirectional composite plate immersed in water has been given in [Mal, et al, 1992]. The ray diagram for some of the early reflections is shown in Figure 12a. Here R^0 indicates the first reflected wave from the top surface of the plate, the rays labeled 1, 2, 3 are associated with the three transmitted waves inside the plate in a decreasing order of their speeds, the rays labeled 11, 12, ..., and 33 are associated with the waves reflected from the bottom of the plate, and T_1, T_2, T_3 indicate the waves transmitted into the fluid through the bottom of the plate. From Snell's law, the velocities V_k, V_l and the angles $?_k$, $?_l$ in the diagram are related through

$$\frac{\sin q}{a_0} = \frac{\sin q_k}{V_k} = \frac{\sin q_l}{V_l} \qquad (6)$$

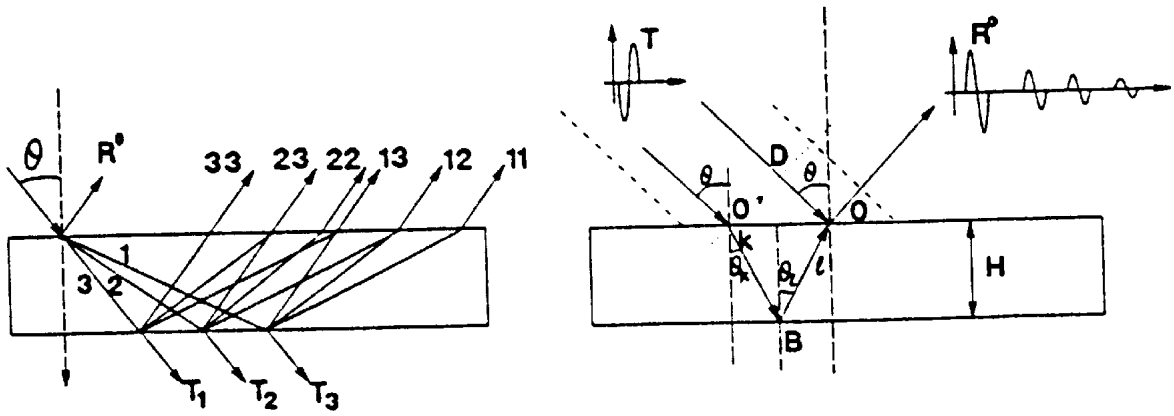

(a) (b)

FIGURE 12: Ray diagram of the reflected waves in a unidirectional composite plate

Two possible ray paths leading to the same point on the receiver are sketched in Figure 12b. The difference in the arrival times, t_{kl}, between rays along paths DO and O′BO can be expressed as

$$t_{kl} = H(z^*_k + z^*_l) \qquad (7)$$

where the normalized slowness $?_k^*$ (= $?_k/?$) is related to the elastic constants; and the details of the derivation of Eq. (7) can be found in Mal, et al [1992], and is omitted here. It should be noted that equation (7) is valid for homogenous waves only, i.e., when $?_k^*$, $?_l^*$ are real. In general, there are three possible bulk wave speeds in a composite material, and the recorded time history should contain a reflected pulse from the top surface followed by nine reflected rays from the bottom of the plate, as well as their multiple reflections. Since the wave speed in a composite material is a function of the orientation f, it is possible to have critical values of f for a fixed value of the incident angle $?$. Thus, some of the homogenous waves may become evanescent when the propagation angle f is larger or smaller than a certain critical angle f_c.

Based on the above theory, an experimental procedure was formulated to determine the five stiffness constants [Mal, et al, 1993]. A summary of the procedures is given below.

a) Pulse-echo test

Using the first pulse, labeled 11, c_{22} can be determined from its travel time from the formula

$$c_{22} = 4rH^2 / t_{11}^2$$

b) Oblique insonification with $f = 90^o$

The constants c_{22} and c_{23} can be determined from the equations

$$c_{22} = \frac{r}{\left(\frac{t_{11}}{2H}\right)^2 + \left(\frac{\sin^2 q}{a_0^{\,2}}\right)}$$

$$c_{23} = \frac{r}{\left(\frac{t_{11}}{2H}\right)^2 + \left(\frac{\sin^2 q}{a_0^{\,2}}\right)} - \frac{2r}{\left(\frac{t_{13}}{H} - \frac{t_{11}}{2H}\right)^2 + \left(\frac{\sin^2 q}{a_0^{\,2}}\right)}$$

c) Oblique insonification with f less than the critical angle f_c.

After c_{22} and c_{23} have been determined, the constant c_{55} can be found as follows. With fixed incident angle $?$, adjust f such that the pulses "22" and "23" can be identified clearly. Then from measured t_{22}, c_{55} can be determined from

d) Oblique insonification with $f = 0^o$

$$c_{55} = \frac{r a_0^{\,2}}{\sin^2 q \cos^2 f}\left\{1 - \frac{c_{22} - c_{23}}{2r}\left[\left(\frac{t_{23}}{H} - \frac{t_{22}}{2H}\right)^2 + \frac{\sin^2 q \sin^2 f}{a_0^{\,2}}\right]\right\}$$

$$c_{11} = \left[\frac{a_0{}^2 c_{22} c_{55}}{r(c_{55}\sin^2 q - r a_0{}^2)\left(\frac{t_{11}}{2H}\right)^2} \left(\frac{t_{12}}{H} - \frac{t_{11}}{2H}\right)^2 + 1 \right] \frac{r a_0{}^2}{\sin^2 q}$$

$$c_{12} = \left\{ (c_{11}c_{22} + c_{55}{}^2) - \frac{a_0{}^2}{\sin^2 q} \left[r(c_{22} + c_{55}) - c_{11}c_{55} \left(\left(\frac{t_{11}}{2H}\right)^2 + \left(\frac{t_{12}}{H} - \frac{t_{11}}{2H}\right)^2 \right) \right] \right\}^{\frac{1}{2}} - c_{55}$$

The remaining two unknowns c_{11} and c_{12}, can be determined from the equations

Since experiment (d) is difficult to carry out due to the small incident angles involved, an alternate method is proposed to determine the remaining constants c_{11} and c_{12}. Our calculations have shown that the reflected field changes significantly near the critical angle [Mal, et al, 1993], and the arrival times of these pulses are strongly affected by c_{11} near the critical angle. We use this critical angle phenomenon to determine the constants c_{11} and c_{12}. Recall that the equation for the bulk wave speed V associated with the constants c_{11} and c_{12} can be written as

$$\left[(a_1 - a_5) + (a_5 - V^2)/n_2^2\right] a_2 - a_3{}^2 + \frac{(a_5 - V^2)^2 + (a_5 - V^2)(-a_5 + a_1 n_2^2) + a_5(a_1 - a_5) n_1^2 n_2^2}{n_1^2 n_2^2} = 0$$

where $n_1 = \cos f$, $n_2 = \sin f$. The constants a_1, a_4, a_5 can be derived from the known constants c_{22}, c_{23}, c_{55}, and the remaining unknowns a_2 and a_3 can be solved and the constants c_{11} and c_{12} can be calculated for two measured critical angles f_c at different incident angles

RESULTS FROM PULSED OBLIQUE INSONIFICATION

Polymer and metal matrix composites were tested to examine the capability of the ultrasonic oblique insonification method as a means to detect defects in them and to determine their material properties. Using the experimental setup and the LLW inversion algorithm described earlier the elastic properties of graphite/epoxy AS4/3501-6 composite using laminate specimens of different thickness. The result for a 24-layer, 3.378 mm thick unidirectional laminate are give in Table 1.

TABLE 1: Inverted stiffness constants for graphite/epoxy AS4/3501-6 $[0]_{24}$ laminate.

? (g/cm^2)	c_{11} (GPa)	c_{12} (GPa)	c_{22} (GPa)	c_{23} (GPa)	c_{55} (GPa)
1.578	166.07	7.09	16.19	7.52	7.79

The values elastic constants determined from this study are within the acceptable range for these materials.

The reflected signals from an acoustic wave incident at 20° on an 8-ply unidirectional GR/EP composite of 1 mm nominal thickness are shown in Figure 13. The polar angles, measured relative to the fibers in the top layer, are different in the three cases shown. For 0° orientation, the reflected pulses emerge sequentially with equal times-of-flight, and the quasi-shear-shear wave yields a series of significant signals with behavior that is similar to an isotropic plate. For off-axis polar orientations, the pulses consist of multiple reflections with unequal times-of-flight. Our calculations have shown that the reflected pulses come from ray paths corresponding to mode-converted bulk waves traveling at different speeds. These waves cause the time delays between the successively arrived signals to be irregular. This is true even for motion on the quasi-isotropic plane ($\varphi = 90^{o}$), in sharp contrast to propagation along the fibers or in isotropic media, where all bulk waves generated at the same surface have equal influence on the reflected signals. Examination of the reflected pulses along various orientations with the fibers for a fixed angle of incidence can be used to identify the polar critical angle. At this angle, a transition is observed in the reflected pulses where the amplitude of the multiple reflections reach a minimum level.

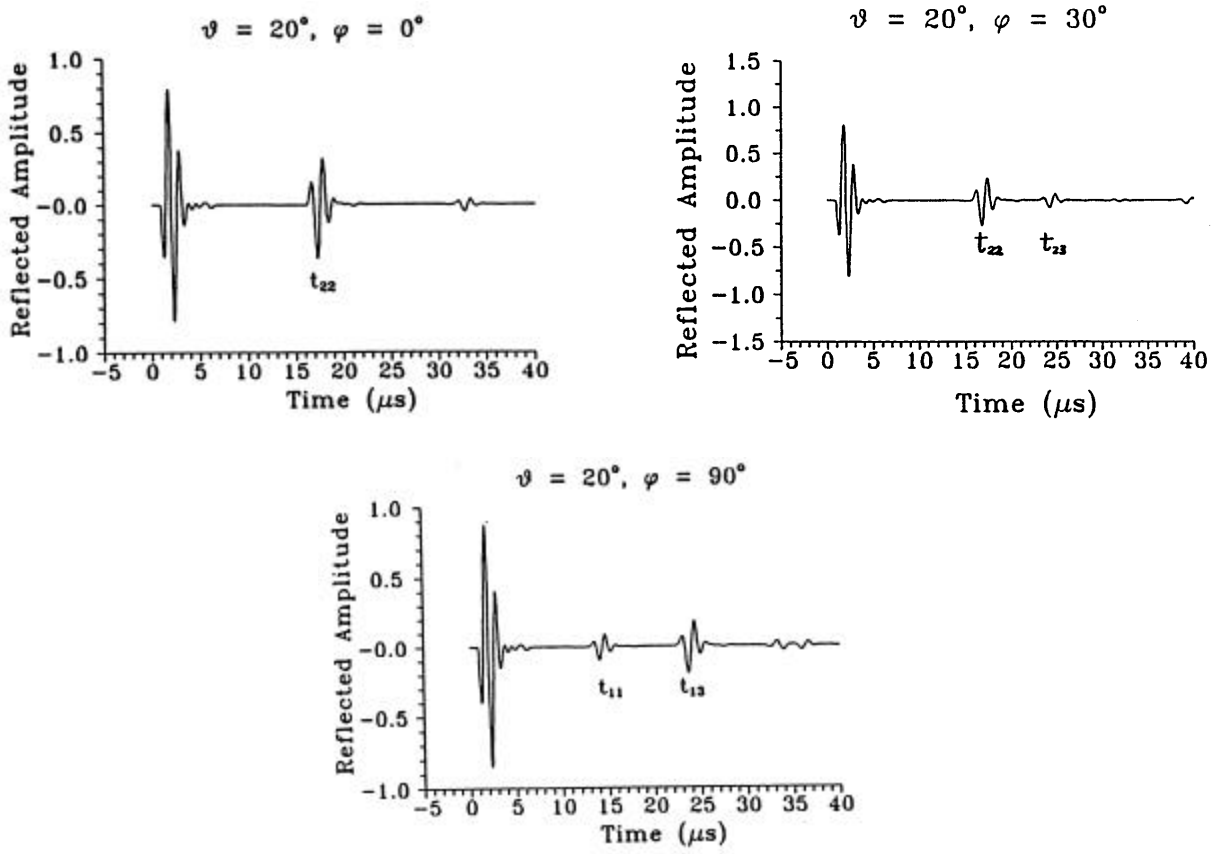

FIGURE 13: Reflected signal from $[0]_8$ laminate at 20° angle of incidence for 0°, 30° and 90° orientations

For propagation in the quasi-isotropic plane, $\varphi = 90^{o}$, only longitudinal or transverse waves are present, as in an isotropic plate. The reflected signal from the fastest longitudinal-longitudinal wave is followed by longitudinal-transverse or transverse-longitudinal wave. The latest arrived signal is from transverse-transverse wave. The reflected pulses due to the individual bulk waves and the top

surface reflection clearly explain the anomalous behavior obtained at off-axis propagation in a unidirectional composite laminate.

It should be noted that the effects of the transducer and other factors related to the experiment are eliminated in this study by convolving the calculated impulse response with a reference reflected pulse from a tungsten film placed over the specimen. The tungsten film produces nearly total reflection of the incident waves and the convolution with the reflected waves from it eliminates the effects of the transducer response and the propagation effects in the fluid medium. The effects of attenuation is included in the theoretical model through the introduction of three dissipation constants [Mal, et al, 1992. The damping constants were varied until a good visual fit of the measured and calculated results could be obtained.

Using pulse-echo data for a unidirectional 3.378 mm thick AS4/3501-6 graphite/epoxy composite the value of c_{22} is found to be 16.3 GPa. The result for incidence at ? = 15° and f = 90° allowed the determination of c_{23} as 7.95 GPa. Testing at ? = 15° and f = 30° allowed to determine c_{55} as 7.74 GPa. The identification of the reflections 22 and 23 requires the use of a relatively low incidence angle; this angle is difficult to obtain experimentally with a single LLW setup. Therefore, this pulse technique was used and two critical angles were identified: f_c = 58.1° for ? = 15°, and f_c = 68.7° for ? = 20°, and thus c_{11} and c_{12} were calculated as 166.05 and 7.06 GPa, respectively. Detailed description of the procedure and the error analysis can be found in [Mal, et al, 1993] and will be omitted.

To produce an image of inherent defects, C-scans were prepared using the LLW setup and pulses as well as tone-bursts. Pulses provided much more effective defects imaging capability than using a single LLW mode in tone-burst. C-scan images were made using pulses where the variables that were examined included the time-of-flight and amplitude. A 24-layer unidirectional graphite/epoxy T300/CG914 laminate was tested at 20° incidence angle along the critical polar angle. The sample was made with series of Teflon foils 25.4, 12.7 and 6.35 mm in diameter and were placed at 1/4, 1/2 and 3/4 of the laminate thickness. At the same depth, an area of 25.4 mm diameter was covered with 40 μm diameter microballoons. To simulate ply-gap, a 6.35 × 12.7 mm cut was made in a single layer at the above three depths along the rows of the simulated-delaminations and -porosity. Examination of the time-domain response from the areas with the simulated defects have shown a response that characterize the particular defect type

Figure 14 presents a C-scan with the variations of the highest signal obtained beyond the specular reflection (first reflection). As shown, all three types of embedded defects - delamination, porosity and ply-gap were clearly identified. Further, the changes of the resin/fiber ratio significantly affected the amplitude. On the other hand, Figure 15 shows a C-scan image presenting the variations of the time-of-flight values for the $[0]_{24}$ sample. Different colors were assigned to the various time-of-flight ranges in order to present the depth of the defects in the sample. The horizontal strips along the C-scan image are parallel to the fiber orientation. Polar backscattering test of these areas indicated a distribution of localized scatterers. Most probable source of such indications is microballons that migrated along the fibers during the laminate cure stage. The depth distribution of the simulated porosity can be identified from the color of the dots representing their reflected signal.

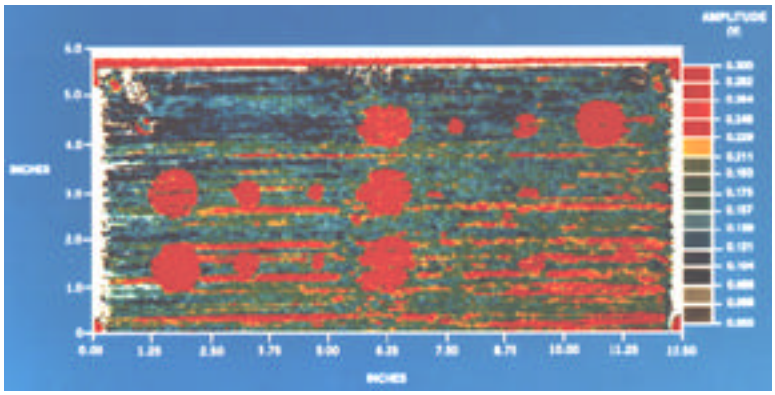

FIGURE 14: Pulsed oblique insonification C-scan showing amplitude variations for a graphite/epoxy $[0]_{24}$ laminate

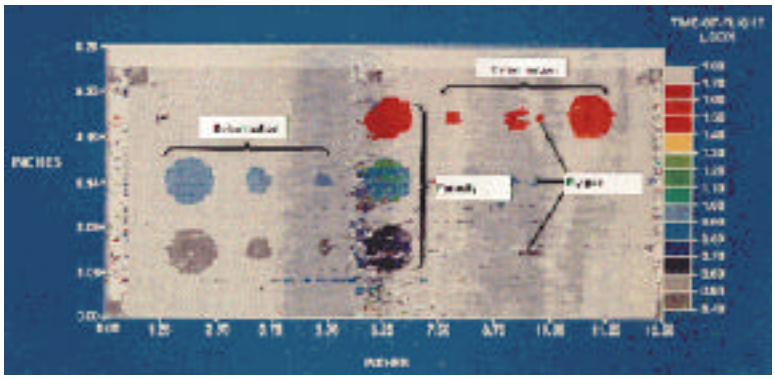

FIGURE 15: Pulsed oblique insonification C-scan showing time-of-flight variations for a graphite/epoxy $[0]_{24}$ laminate

CONCLUDING REMARKS

The leaky Lamb wave (LLW) method has been studied by numerous investigators during the last decade and this has resulted in a good quantitative understanding of the behavior of the waves in composite materials. However, this knowledge base has yet to be translated into the development of practical NDE methods for field applications. The issues that need to be addressed for making further progress can be summarized below.

1. Material density - The inverted material constants are based on the assumption that the material density is known. This assumption may not be accurate, particularly in the presence of flaws. Although radiographic testing can be used to determine the density nondestructively, such tests are uneconomical and require access from two sides of the test structure. Augmentation of the capability of the LLW technique to determine the density of the material nondestructively using access from a single side.
2. Multi-orientation laminates - The inversion algorithm developed for the determination of the elastic properties has been very successful for unidirectional laminates. Analysis of laminates with multi-orientation layers using ply-by-ply analysis is complex and leads to ill-posed inversion problems. Methods of inverting the material elastic properties without the necessity to deal with individual layers are needed and are currently being explored [Shih, et al, 1998] using contact type tests. Extension of the LLW data inversion to determine the laminate stiffness constants and their in-service degradation for arbitrary orientation and number of layers is desirable.

a) Data acquisition - The current LLW data acquisition setup is complex and not very user friendly. Significant improvement of the data acquisition process has recently been made by

automating the process of aligning the height of the setup as discussed above. Also, the use of the polar backscattering technique [Bar-Cohen and Crane, 1982] polar angle has made the polar angle alignment more precise. However, development of user-friendly software is needed to allow interactive control of the system, minimizing the need for manual setup and alignment.

3. Time-consuming process - The formerly reported process of acquiring dispersion curves was time consuming, taking between 10 and 20 minutes to acquire a curve for a single point on a composite material. The procedures described here have been helpful in speeding up the acquisition of dispersion data significantly. Continued improvements in the speed of data acquisition and analysis would increase the practical applicability of the LLW method in field environments.

ACKNOWLEDGMENT

The research at Jet Propulsion Laboratory (JPL), California Institute of Technology, was carried out under a contract with National Aeronautics Space Agency (NASA).

REFERENCES

Balasubramanian K., and J. Rose, "Physically Based Dispersion Curve Feature Analysis in the NDE of Composite Materials," Research in NDE, Vol. 3, No. 1 (1991), pp. 41-67.

Bar-Cohen, Y., and R. L. Crane, "Acoustic-Backscattering Imaging of Subcritical Flaws in Composites," *Materials Evaluation*, Vol. 40, No. 9 (1982), pp. 970-975.

Bar-Cohen Y., and D. E. Chimenti, "Leaky Lamb Waves in Fiber-Reinforced Composite Plates," Review of Progress in Quantitative NDE, Vol. 3B, D. O. Thompson and D. E. Chimenti (Eds.), Plenum Press, New York and London (1984), pp. 1043-1049.

Bar-Cohen Y., A. K. Mal and C. -C. Yin, "Ultrasonic Evaluation of Adhesive Bonding," Journal of Adhesion, Vol. 29, No. 1-4, (1989), pp. 257-274.

Bar-Cohen, Y., et al, "Ultrasonic Testing Applications in Advanced Materials & Processes," *Nondestructive Testing Handbook*, Section 15 in Vol. 7: Ultrasonic Testing, Section 8, A. Birks and B. Green Jr. (Ed.), American Society for NDT, Columbus, OH (1991), pp. 514-548.

Bar-Cohen, Y., A. Mal, and S.-S. Lih, "NDE of Composite Materials Using Ultrasonic Oblique Insonification, *Materials Evaluation*, Vol. 51, No. 11, (1993), pp.1285-1295.

Bar-Cohen Y., and P. Backes, "Open-architecture robotic crawlers for NDE of aircraft structures," *Materials Evaluation*, Vol. 57, No. 3 (1999), pp. 361-366.

Buchwald, V. T., "Rayleigh Waves in Transversely Isotropic Media," Quarterly J. Mechanics and Applied Mathematics, Vol. 14 (1961), pp. 293-317.

Christensen, R. M., "Mechanics of Composite Materials," Chapter 4, Wiley, New York (1981).

Dayal, V., and V.K. Kinra, "Leaky Lamb waves in an anisotropic plate. I: An exact solution and experiments," *J. Acoustic Soc. of Amer.*, Vol. 85, No. 6, (1989), pp. 2268 – 2276.

Jansen D. P., and D. A. Hutchins, "Lamb wave immersion Topography," Ultrasonics, Vol. 30 (1992), pp. 245-254.

Karim, M.R., Mal, A.K. and Bar-Cohen, Y., "Inversion of Leaky Lamb Wave Data by Simplex Algorithm," *J. Acoust. Soc. Am.*, Vol. 88, (1990), pp. 482-491.

Mal, A.K. and Singh, S., *Deformation of Elastic Solids*, Prentice Hall, 1991.

Mal, A. K., "Wave Propagation in Layered Composite Laminates under Periodic Surface Loads." *Wave Motion*, Vol. 10, (1988), PP. 257-166.

Mal, A. K., and Y. Bar-Cohen, "Ultrasonic Characterization of Composite Laminates," *Proceedings of the Joint ASME and SE meeting*, AMD-Vol. 90, A. K. Mal and T.C.T. Ting (Eds.), ASME, NY, (1988), pp. 1-16.

Mal, A. K., C. -C. Yin, and Y. Bar-Cohen, "Ultrasonic NDE of Cracked Composite Laminates," *Composites Engineering, Pergamon Press*, Vol. 1, No. 2, (1991), pp. 85-101.

Mal, A.K., Bar-Cohen, Y. and Lih, S.-S., "Wave Attenuation in Fiber-Reinforced Composites," *Proceedings of M^{3}D*, Kinra, V.K. (editor), ASTM STP, Vol. 1169, (1992), pp. 245-261.

Mal, A.K., Yin, C.C. and Bar-Cohen, Y., "Analysis of Acoustic Pulses Reflected from Fiber-Reinforced Composite Laminates," *J. Appl. Mech*., Vol. 59, pp. 136-144, 1992

Mal A. K., S.-S. Lih and Y. Bar-Cohen, "Nondestructive Characterization of the Elastic Constants of Fiber Reinforced Composites," Proceedings of the 34th AIAA/ASME/ASCE/AHS/ASC Structures, Structural dynamics and Materials Conference, Part 1, AIAA-93-1349-CP, held in La Jolla, CA, April 19-22 (1993), pp. 472-484.

Nagy P. B., W. R. Rose and L. Adler, "A Single Transducer Broadband Technique for Leaky Lamb Wave Detection," Review of Progress in QNDE, Vol. 6A (1987), pp. 483-490.

Nayfeh, A. H., and D. E. Chimenti, "Propagation of Guided-Waves in Fluid-Coupled Plates of Fiber-Reinforced Composite," Journal of the Acoustical Society of America, Vol. 83, No. 5 (May 1988), pp. 1736-1747.

Rohklin S. I., and W. Wang, "Critical Angle Measurement of Elastic Constants in Composite Materials," J. Acoustic Society of America, Vol. 85, No. 5 (1989), pp. 1876-1882.

Shih, J.-H, Mal, A.K. and Vemuri, 1998] M., "Plate Wave Characterization of Stiffness Degradation in Composites During Fatigue," *Research in Nondestructive Evaluation*, Vol. 10, (1998), pp 147-162.